Gait Measurement System Toward Robotic Rehabilitation of Locomotive Functions

Ryo Saegusa
Dept. of Robotics & Mechatronics
Kanagawa Institute of Technology
Atsugi, Japan
ryo.saegusa@syblab.org

***Abstract*—The extension of health expectancy is getting a more important subject for developed countries with higher rate of elderly population. In order to sustain their societies, aged people are encouraged to participate in the social activities, while the social participation requires them to keep their locomotive function high enough to accomplish their missions. From this reason, the easy and frequent assessment of the locomotive function thought the people's daily lives is strongly expected. One of the promising methods to evaluate locomotive function is the Timed Up and Go test (TUG test), which is a widely used method in the field of physical therapy for locomotive rehabilitation in medical facilities. Throughout our research activities, we have been investigating robotic approaches to assess cognitive and motor functions of aged people in the purpose of their health expectancy extension. In this article, we will propose a novel method of a gait measurement system that will be incorporated with health care mobile robots developed previously. We demonstrated experiments to measure the walking patterns of 23 subjects of aged people in order to evaluate their locomotive functions using the proposed gait measurement system.**

***Index Terms*—Gait Measurement, TUG Test, Health Care Robot**

I. Introduction

The extension of health expectancy is getting a more important subject for developed countries with higher rate of elderly population. In order to sustain their societies, aged people are encouraged to participate in the social activities, while the social participation requires them to keep their locomotive function high enough to accomplish their missions. From this reason, the easy and frequent assessment of the locomotive function thought the people's daily lives is strongly expected. One of the promising methods to evaluate locomotive function is the Timed Up and Go test (TUG test), which is a widely used method in the field of physical therapy for locomotive rehabilitation. The advantage of the TUG test is the simplicity in its measurement, where it requires only a stop watch. In this measurement, however, important features that appear in body movements are not extracted well. The latest robotic technology is expected to be applied for the measurement.

In literature, gait training platforms such as power assisting libs and body supporting mobile platforms have been studied well [1] [2]. These types of platforms are effective for physically supporting aged people and patients with muscle-originated locomotive problems. On the other hand, patients in nerve-originated locomotive problems such as cerebral stroke and Parkinson disease rather requires cognitive assistance and intuitive navigation to recover smooth and periodicity body movements [3] [4]. Cognitive advantage of robotic assistance in rehabilitation is not fully discussed.

In our research, we firstly develop and examine a stationary device for the gait measurement system, and then port the functionality of the gait measurement into the mobile robot to allow more dynamic use of the gait measurement. Figure 1

This research was supported by the KAIT Advanced Technology Research Center (research project III, 2020-2023).



Fig. 1. A stationary device for the gait measurement (left) and the TUG test course (right).



Fig. 2. Lucia, a human-interactive health care robot.

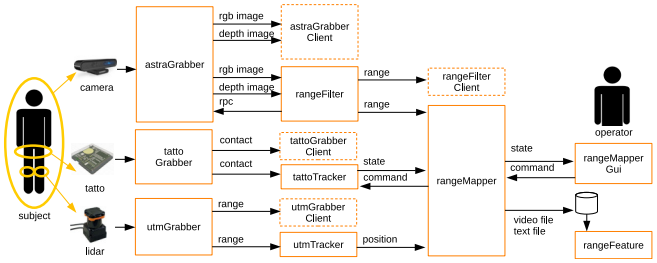


Fig. 3. The architecture of the gait measurement system.

shows the stationary device for the gait measurement system that we developed. We demonstrated experiments of TUG tests to measure the walking patterns of 23 subjects of aged people in order to evaluate their locomotive functions. We also performed experiments of the gait measurement using the health care mobile robot. Figure 2 shows Lucia, a human-interactive health care mobile robot. Lucia is capable of human interaction using locomotion and stimulation function on audio, visual and somatosensing.

II. Method

A. Gait measurement system

The gait measurement system that we propose here is an integrated optical measurement system that captures a temporal sequence of human locomotive movements in the context of the TUG tests, and then extracts features to be useful for the assessment of locomotive function. The locomotive movements captured by the system includes several elements of motions that frequently appear in the activity of our daily lives. In the system, the elements of motions are labeled with the names of *stand-up* motion, *outward-gait* motion, *circular-gait* motion, *return-gait* motion and *sit-down* motion. These five elements of motions are automatically segmented based on the video streams given by a depth camera. The temporal durations of the motions are then recorded. Meanwhile, the spatial movements of left and right legs are also tracked based on the field scanning given by a LiDAR sensor. The trajectories of the legs are recorded as well. The start and end of the measurement is automatically detected by Tatto, a seat sensor device that we designed and developed originally. Figure 3 shows the architecture of the gait measurement system.

B. Camera-based motion segmentation

The automatic segmentation of the five elements of motions is realized by the sequential processes of video capturing, 3D reconstruction, extraction of spacial features, and pattern fittings. In the video capturing, the image streams of RGB frames and depth frames are captured. The surface of the human subject walking inside the cuboid volume of the TUG domain is extracted from the image streams and represented in the 3D Cartesian coordinate system as point clouds with color textures. Equations (1) represent

TABLE I
Notations of variables.

notation	parameter	value [unit]
θ_h	horizontal angle of FOV	60.0 [deg]
θ_v	vertical angle of FOV	49.5 [deg]
θ_d	diagonal angle of FOV	73.0 [deg]
θ_{hh}	half horizontal angle of FOV	30 π / 180 [rad]
θ_{vh}	half vertical angle of FOV	24.75 π / 180 [rad]
θ_{dh}	half diagonal angle of FOV	36.5 π / 180 [rad]
$\theta_x(x)$	half horizontal angle of target (x,y)	[rad]
$\theta_y(y)$	half vertical angle of target (x,y)	[rad]
$\theta_z(x,y)$	half diagonal angle of target (x,y)	[rad]
w	width of image frame	640 [px]
h	height of image frame	480 [px]
w_h	half width of image frame	320 [px]
h_h	half height of image frame	240 [px]
x	horizontal image coordinate of target from image center	[px]
y	vertical image coordinate of target from image center	[px]
d	depth on of target (x,y)	[mm]
$X(x,y,d)$	horizontal (left to right) coordinate of physical space	[mm]
$Y(x,y,d)$	vertical (bottom to top) coordinate of physical space	[mm]
$Z(x,y,d)$	depth (near to far) coordinate of physical space	[mm]
$Y_h(t)$	vertical (bottom to top) coordinate of the highest point at time t	[mm]
$Z_n(t)$	horizontal (near to far) coordinate of the nearest point at time t	[mm]
t	time	[s]

the transformation from the image coordinates (x, y) to the visual angle $(\theta_x, \theta_y, \theta_z)$. Equations (2) represent the transformation from the visual angle $(\theta_x, \theta_y, \theta_z)$ to the Cartesian coordinates (X, Y, Z).

$$\begin{aligned} \tan\theta_x(x) &= \tan\theta_{hh}\left(\frac{x}{w_h}\right), \\ \tan\theta_y(y) &= \tan\theta_{vh}\left(\frac{y}{h_h}\right), \\ \tan\theta_z(x,y) &= \tan\theta_{dh}\left(\frac{\sqrt{x^2+y^2}}{\sqrt{w_h^2+h_h^2}}\right). \end{aligned} \tag{1}$$

$$\begin{aligned} X(x,y,d) &= -\frac{d\tan\theta_x}{\sqrt{1+\tan^2\theta_x}}, \\ Y(x,y,d) &= -\frac{d\tan\theta_y}{\sqrt{1+\tan^2\theta_y}}, \\ Z(x,y,d) &= \frac{d}{\sqrt{1+\tan^2\theta_z}}. \end{aligned} \tag{2}$$

$$\begin{aligned} Y_h(t) &= \max_{i\in p.c.} Y_i(t), \\ Z_n(t) &= \min_{i\in p.c.} Z_i(t). \end{aligned} \tag{3}$$

Figure 4 shows a course of the TUG test and the procedure of segmentation. From this point cloud data, the highest point in the domain $Y_h(t)$ and the nearest point $Z_n(t)$ to the sensor are extracted as represented in Eq. (3), where they correspond to the head top and body front of the walking subject, respectively. The time series of these 3D positions are recorded, then. From the time series of the body front

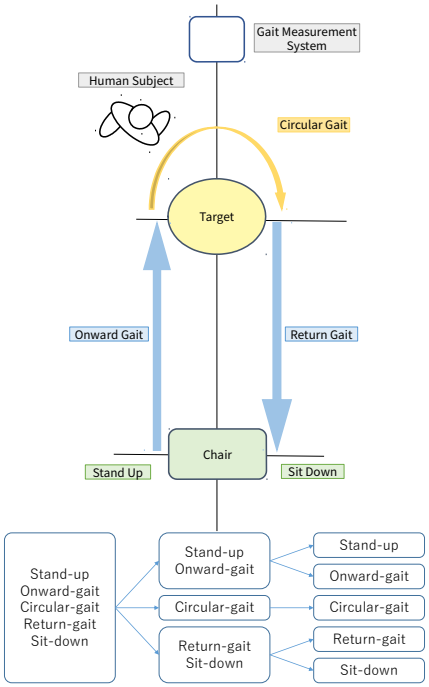


Fig. 4. A course of the TUG test and the procedure of segmentation.

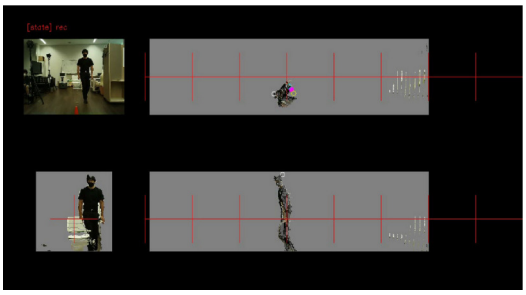


Fig. 5. 3D Visualization of full body movements from the front, side and top view points.

position, the target *circular-gait* motion is segmented, where the system estimates the relative positions between the target to go around and the subject body. From the time series of the head top position, the *stand-up* motion is segmented from the *onward-gait* motion, while the *sit-down* motion is segmented from the *return-gait* motion. The system detects the segments of the *stand-up* motion and *sit-down* motion based on the piece-wise linear fitting for the head motion patterns. Figure 5 shows the 3D visualization of whole body movements from the front, side and top view points.

C. LiDAR-based leg tracking

The tracking of spacial movements of legs are realized by the sequential processes of field scanning, 2D reconstruction, and extraction of leg positions. In the field scanning, the LiDAR sensor scans the horizontal plane in the TUG domain at the slightly lower level of knee joints. The scanned data

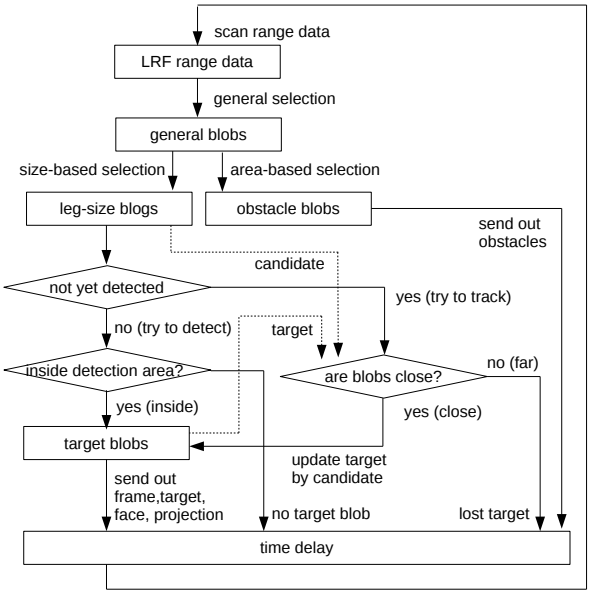


Fig. 6. The algorithm flow of blob detection.

are represented in the 2D Cartesian coordinate systems as point clouds. From these point clouds, two arch shapes are extracted, where they are corresponding to the horizontal slices of the left and right lower legs of the walking subject. The time series of the 2D center positions of the legs are recorded. From the time series of the lower leg positions, a set of a stance phase and a swing phase is segmented as a single period of the steps. These lower leg positions are then represented in the 3D Cartesian system together with the point clouds of the subject body.

In order for leg tracking, we implemented fast blob detection algorithm based on the distance range. The algorithm sequentially compares the distance gap of adjacent angle and segments the angle domain if the distance gap is over threshold, e.g. 50mm. The system handles each segment as a general blob. Figure 6 shows the flow chart of blob detection. Firstly, general blobs are filtered by size-based selection and area-based selection. The selected blobs are regarded as leg-size blob and obstacle blob, respectively. Secondly, a newly detected pair of leg-size blobs is defined as target legs to track. The system keeps leg tracking as long as one leg is visible. The tracking is done based on the distance from the linearly estimated target position and candidate blobs.

A leg movement is modeled with a finite state machine (FSM). Figure 7 shows a state transition of the leg movement. The FSM is composed of three states that are the idle S_0, stance S_1 and swing S_2 states. The S_0 is the initial state of the FSM before the system starts leg tracking or after the tracking legs are lost. The S_1 is the state of stance when the training subject is standing and before lifting a leg up. The S_2 is the state of swing while the leg is moving. The condition of the state transition from S_1 to S_2 is defined as the case that $\Delta x > \Delta x_L$, where x denotes the coordinates

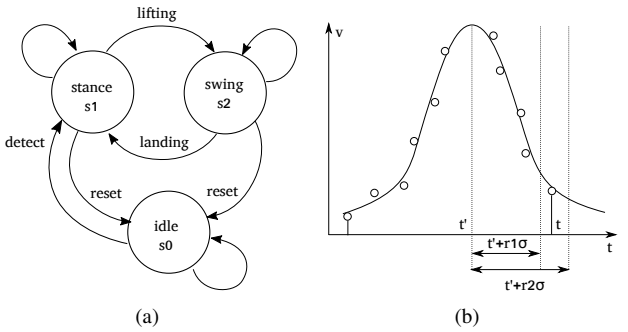


Fig. 7. State transition of leg movements. (a) a finite state machine model. (b) Velocity profile of the tracking leg.

to the absolute direction of gait. Δx is defined as follows:

$$\Delta x = |x(t) - x(t - t_1)|, \tag{4}$$

where t and t_1 denote the current time and the time when the FSM most recently transited the state into S_1. Δx therefore means the spatial variance from the previously stepped position. Δx_L denotes a threshold of spatial movements. The condition of the state transition from S_2 to S_1 is defined as the case that the velocity of the tracking leg is decaying. Figure 7(b) shows the velocity profile of the tracking leg. When the state is S_2, the FSM evaluates the velocity profile of the tracking leg v with the function f:

$$f(v(t)) = G(v(t); \bar{t}, \sigma, a, b), \tag{5}$$

$$v = |(v_x(t), v_y(t))|, \tag{6}$$

where G is the Gaussian function with the center $\bar{t}$, variance σ, amplitude a and bias b. These function parameters are given by non-linear optimization with the frame data set of $\{v_1, \cdots v_n\}$. If the current time is in the domain between $(\bar{t}+r_1\sigma)$ and $(\bar{t}+r_2\sigma)$, the FSM considers that the tracking leg is going to land on the floor, and transits the state from S_2 (swing) to S_1 (stance). r_1 and r_2 are the parameters to control the landing detection.

D. Illuminance-based standing detection

The start and end of walking in the TUG test is automatically detected by Tatto, a seat sensor device that we designed and developed originally. Figure 8 shows the appearance of the inside and the outside of the Tatto, and a sample plot of temporal sequences measured by Tatto. In the plot, the horizontal and vertical axis indicate the time and illuminance level. Tatto is set on a chair to detect the timing of sitting and standing of a person. The detection principle is based on the ambient illuminance of the environment. If the ambient illuminance on the chair is shielded by a person who sits down on the chair, the sitting state is detected by comparing a threshold illuminance level that can be calibrated in advance.

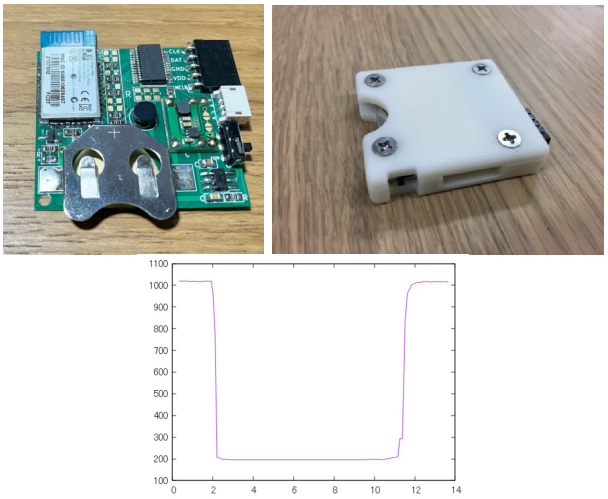


Fig. 8. The appearance of the inside (up left) and the outside (up right) of a seat sensor Tatto, and a sample plot of temporal sequences (bottom).

E. Robotic applications

The functionality of the stationary device is ported into Lucia shown in Fig.2 to allow the gait measurement system in dynamic environments by using its mobility. Visual projection, sound generation and local body vibration equipped with in the robot intuitively inform training subjects of the current state of own movements and the next target in the middle of motor execution. We hypothesized that enhancement of own motor recognition leads efficiency for recovery of motor control in rehabilitation. We implemented a interactive robot system to realize the motor recognition.

In early studies, robotic guidance using visual projectors were proposed, where the projector was mounted on a pan-tilt unit of the mobile base [5] [6]. The step-on interface with a projector was proposed, where the robot projected footprints for users walk guidance [7] [8]. In addition to visual stimulation, auditory stimulation is effective for motor recognition. Rhythm sound presentation is effective for locomotive rehabilitation [9] [10] [11]. The auditory stimulation mediates entrainment between the system and human subject in the walking task [12]. Comparing with the conventional studies, this study focuses on the enhancement of motor recognition. The enhancement of the motor recognition will be realized by the closed loop of interaction between the robot and training subject based on measurement, motor planning, sensory stimulation and locomotion.

III. Experiments

A. Motion segmentation of aged people

We demonstrated experiments to measure the walking patterns of 23 subjects of aged people (all female subjects in 70s or 80s) in order to evaluate their locomotive functions using the proposed gait measurement system. For simplicity of the experiments, we used a skeleton device shown in Fig. 1. The skeleton device is the subset version of the

Lucia shown in the Fig. 2. In advance of the experiments, we requested the subjects to answer a questionnaire that asks about the experience of falling down in their daily lives, and divide the subjects into the two groups denoted as the Group A and Group B. The Group A is consist of members who have experiences of actual falling down or almost. The Group B is consist of members who have no experience of falling down. Table II represents the contents of the questionnaire and Table III represents the results of the questionnaire, respectively. The subjects who chose the answer (1) or (2) in A3 were assigned to the Group A, while the subjects who chose the answer (3) in A3 were assigned to the Group B. Table III shows the results of each group separately. The result of the questionnaire suggested that the members of the Group have tendency to feel dangers more than the members of the Group B. The members of the Group A especially feel dangers in stepping, which is the most critical factor to cause actual falling down.

Next, we performed analysis of features in the TUG test data sampled from the subjects. Figure 9 shows the results of motion segmentations. In the figure, No.2070 and No.2001 are the members of the Group A and Group B, respectively. The plots show the representative patterns of their belonging group. As shown in the figure, the motion segmentation functioned successfully, and output the set of time durations required for respective five motions. Table IV summarized the set of the time durations of the Group A and Group B, respectively. In the results, the set of duration times seemed similar in average, and we could not find a clear correlation between the time durations of motions in the TUG test to the experience of falling down. In the individual level, however, we found the high variance of the time duration especially in the *sit-down* motion, and that caused the latency in the TUG test. This result suggests the possibility of the *sit-down* motion for the assessment of locomotive function. The *sit-down* motion is considered to require high confidence of landing on a spot and motor control should correctly stop the whole body motion at the appropriate timing.

TABLE II
CONTENTS OF THE QUESTIONNAIRE.

Q1.	Have you felt a danger to fall down in the following situations? Choose all the items that apply.
A1.	(1) Standing up (2) Walking straightly (3) Shifting direction (4) Sitting down (5) Stepping on a different level (6) Walking up on a slope
Q2.	What do you think the reasons of feeling are in Q1 ? Choose all the items that apply.
A2.	(1) Stamble (2) Unsteady (3) Slip (4) Misstep
Q3.	Have you fallen down actually? Choose a single item that applies.
A3.	(1) Yes actually (2) Not actually, but almost (3) No

TABLE III
RESULTS OF THE QUESTIONNAIRE.

Que.	Answer	# of (A)	Rate (A)	# of (B)	Rate (B)
Q1.	(0) Nothing	4	0.333	7	0.500
	(1) Standing	1	0.083	0	0.000
	(2) Straight	1	0.083	2	0.143
	(3) Direction	0	0.000	2	0.143
	(4) Sitting	0	0.000	0	0.000
	(5) Stepping	5	0.417	3	0.214
	(6) Slope	1	0.083	0	0.000
Q2.	(0) Nothing	5	0.385	10	0.625
	(1) Stamble	3	0.231	2	0.125
	(2) Unsteady	1	0.077	3	0.188
	(3) Slip	2	0.154	0	0.000
	(4) Misstep	0	0.000	1	0.063

B. Leg tracking of disordered gait patterns

We examined the effectiveness of the leg tracking for healthy and disordered gait patterns simulated by physical therapists. In this experiment, we used the Lucia shown in Fig. 2 for the gait measurement. In the experiment, physical therapists who dedicated in gait rehabilitation demonstrated three types of representative gait patterns that appear in the gait of healthy, hemiplegia and aged people. The Lucia measured the gait patterns and analyzed them. The gait patterns of hemiplegia patients and aged people show characteristics in asymmetry gait and short stride gait, respectively. In this experiment, Lucia was set stationary and the subjects walked towards Lucia from the start area that was about 7m away.

Figure 10 shows the velocity profiles of the left and right legs with landing detection. In each case of gait patterns, legs were well tracked and steps were almost correctly detected. Note that the tracking was available over 10m. Moreover, the landing detection did not matter short strides and asymmetric movements towards the side direction. The accuracy of location in the long range tracking is an advantage of LRF-based tracking, compared to the IR-based tracking system. The landing detection functioned successfully. It is considered that the finite state modeling and velocity profile fitting allow noise reduction in estimation of the landing timing.

IV. CONCLUSION

In this article, we proposed a novel method of a gait measurement system that is incorporated with health care mobile robots developed previously. We demonstrated experiments to measure the walking patterns of 23 subjects of aged people in order to evaluate their locomotive functions using the proposed gait measurement system, and successfully analyzed the motion segments appeared in the TUG test. We also examined leg tracking for the healthy and disordered gait patterns. Through the experiment, the features of hemiplegia patients and aged people are well extracted. In the future, we will make use of Lucia to go round in

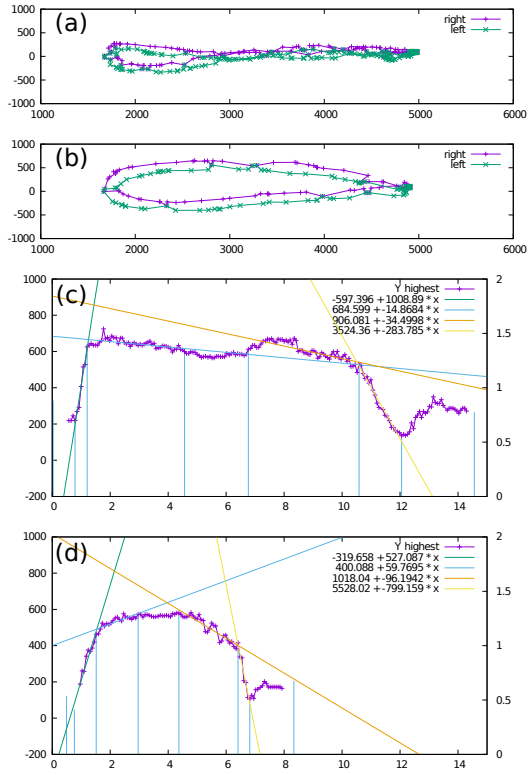


Fig. 9. Trajectories of left and right legs, and motion segmentations based on the profiles of the head top positions. (a) trajectories (No.2070), (b) trajectories (No.2001), (c) motion segments (No.2070), (d) motion segments (No.2001).

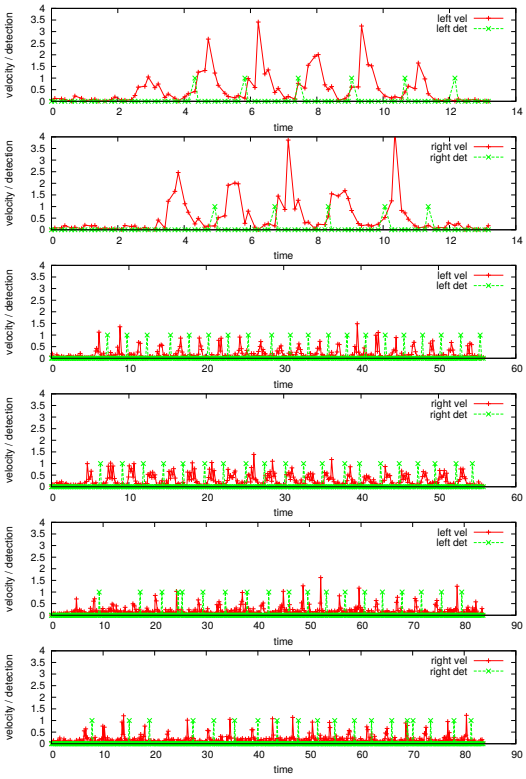


Fig. 10. Velocity profiles of the left and right legs of healthy (top 2 plots), hemiplegia (middle 2 plots) and aged subjects (bottom 2 plots).

TABLE IV
TIME DURATION REQUIRED FOR EACH MOTION.

Type	Group	Sta.	Out.	Cir.	Ret.	Sit.
Ave.	A	0.945	1.85	1.38	2.33	2.37
Dev.	A	0.150	0.692	0.389	0.945	0.789
Ave.	B	0.949	1.86	1.42	2.21	2.50
Dev.	B	0.165	0.251	0.186	0.640	1.01

day-service facilities and assess locomotive functions of the facility users.

ACKNOWLEDGEMENT

We would like to thank Mr. Riku Sudou, Kanagawa Institute of Technology, Ms. Misaki Gemma, Ms. Mayako Nakajima and Prof. Kayo Ogawa, Japan Women's University for their support in experiments and device assembly.

REFERENCES

[1] H. Kawamoto and Y. Sankai, "Power assist method based on phase sequence and muscle force condition for hal," *Advanced Robotics*, vol. 19, no. 7, pp. 717–734, 2005.

[2] A. M. Moseley, A. Stark, I. D. Cameron, and A. Pollock, "Treadmill training and body weight support for walking after stroke," *Stroke*, vol. 34, no. 12, pp. 3006–3006, 2003.

[3] J. Verghese, R. B. Lipton, C. B. Hall, G. Kuslansky, M. J. Katz, and H. Buschke, "Abnormality of gait as a predictor of non-alzheimer's dementia," *New England Journal of Medicine*, vol. 347, no. 22, pp. 1761–1768, 2002.

[4] L. M. Allan, C. G. Ballard, D. J. Burn, and R. A. Kenny, "Prevalence and severity of gait disorders in alzheimer's and non-alzheimer's dementias," *Journal of the American Geriatrics Society*, vol. 53, no. 10, pp. 1681–1687, 2005.

[5] T. Shiotani, K. Maegawa, K. Iwamoto, and J. Lee, "Building a behavior model for the ubiquitous display to be used in a large-scale public facility," in *2012 9th International Conference on Ubiquitous Robots and Ambient Intelligence (URAI)*, 2012.

[6] K. Maegawa, T. Shiotani, K. Iwamoto, T. Noguchi, M. Kasetani, and J.-H. Lee, "Ubiquitous display 2.0: Development of new prototype and software modules for improvement," in *2013 10th International Conference on Ubiquitous Robots and Ambient Intelligence (URAI)*. IEEE, 2013, pp. 102–107.

[7] T. Matsumaru and K. Akai, "Functions of mobile-robot step-on interface," *Journal of Robotics and Mechatronics*, vol. 21, no. 2, p. 267, 2009.

[8] T. Matsumaru and K. Akai, "Step-on interface on mobile robot to operate by stepping on projected button," *Open Automation and Control Systems Journal*, vol. 2, pp. 85–95, 2009.

[9] G. C. McIntosh, S. H. Brown, R. R. Rice, and M. H. Thaut, "Rhythmic auditory-motor facilitation of gait patterns in patients with parkinson's disease." *Journal of Neurology, Neurosurgery & Psychiatry*, vol. 62, no. 1, pp. 22–26, 1997.

[10] M. Suteerawattananon, G. Morris, B. Etnyre, J. Jankovic, and E. Protas, "Effects of visual and auditory cues on gait in individuals with parkinson's disease," *Journal of the neurological sciences*, vol. 219, no. 1, pp. 63–69, 2004.

[11] E. v. Wegen, I. Lim, C. d. Goede, A. Nieuwboer, A. Willems, D. Jones, L. Rochester, V. Hetherington, H. Berendse, J. Zijlmans *et al.*, "The effects of visual rhythms and optic flow on stride patterns of patients with parkinson's disease," *Parkinsonism & related disorders*, vol. 12, no. 1, pp. 21–27, 2006.

[12] H. Takanashi and Y. Miyake, "Co-emergence robot walk-mate and its support for elderly people," *Transactions-society of Instrument and Control Engineers*, vol. 39, no. 1, pp. 74–81, 2003.